Preliminary Exam

Peter Maginot
Co-Chairs: Jim Morel and Jean Ragusa
Committee Members: Marvin Adams and Jean-Luc Guermond

Texas A&M University- Department of Nuclear Engineering

March 31, 2014

Dissertation Goal

Methods for high-fidelity S_N radiative transfer simulations

Requirements to Achieve Goal

1. Accurate Spatial Discretization
   - Higher degree trial space DFEM
   - Must address robustness
2. Accurate Spatial Treatment of Opacities
   - Cell-wise constant is a poor approximation for problems of interest
3. Efficient / Effective Acceleration
   - Computationally efficient
   - Compatible with spatial discretization

Outline

DFEM Discretization

When we discretize the 1-D slab, mono-energetic, neutron transport equation with DGFEM, we get:

$$\mu_d \mathbf{L}\vec{\psi}_d + \sigma_t \mathbf{M}\vec{\psi}_d = \frac{\sigma_s}{2}\mathbf{M}\vec{\phi} + \vec{q}_d + \psi_{in}\vec{f}$$

where we define the following (focusing only on $\mu_d > 0$):

$$\begin{aligned}
\mathbf{L}_{ij} &= B_i(1)B_j(1) - \int_{-1}^{1} \frac{dB_i}{ds} B_j(s)\ ds \\
\mathbf{M}_{ij} &= \frac{\Delta x}{2}\int_{-1}^{1} B_i(s)B_j(s)\ ds \\
\vec{f}_i &= B_i(-1) \\
\vec{q}_{d,i} &= \frac{\Delta x}{2}\int_{-1}^{1} B_i(s)q_d(x)\ ds
\end{aligned}$$

Matrix Lumping

1. One method to improve the "robustness"
   - solution positivity and resistance to oscillations
2. Lumping- makes diagonal mass matrices, does not guarantee change in robustness
3. Two ways to lump mass matrices
   - Collapse an exactly integrated matrix's entries to the main diagonal
   - Use quadrature restricted to the DFEM interpolation points
4. Both methods are equivalent for linear DFEM

Self-Lumping Concept

Since B_i are interpolatory, restricting quadrature to the DFEM interpolation points creates a diagonal mass matrix *automatically*

Self-lumping (SL) $\mathbf{M}$

$$\mathbf{M}_{ij} = \begin{cases} \frac{\Delta x}{2} w_i & i = j \\ 0 & \text{otherwise} \end{cases}$$

- Typically, s_j are chosen as equally-spaced points, and $\mathbf{L}$ and $\mathbf{M}_\sigma$ are integrated analytically
- No requirement that s_j be equally-spaced, could use more accurate quadrature as the interpolation points
  - E.g. Gauss-Legendre (Gauss) or Lobatto-Gauss-Legendre (Lobatto)

Numerical Schemes

New to Dissertation

- Self-lumping with higher degree trial spaces
- Non equally-spaced interpolation points

- **SL Gauss**: Gauss quadrature as interpolation points, quadrature restricted to interpolation points
- **SL Lobatto**: Lobatto quadrature as interpolation points, quadrature restricted to interpolation points
- **SL Newton-Cotes**: Equally-spaced points, quadrature (closed Newton-Cotes) restricted to interpolation points
- **TL** (Traditional Lumping): Equally-spaced points, analytic integration, then collapse to main diagonal
- **Exact DFEM**: Equally-spaced points, analytic integration

Test Problem

Source-free pure absorber, left incident flux, $\psi_{in,d}$, vacuum right BC.
Defining h:

$$h = \frac{\sigma_t \Delta x}{\mu_d}$$

Analytic solution is

$$\psi(x, \mu_d) = \psi_{in,d} \exp[-h]$$

New Results (M&C 2013)

Positivity

- SL Gauss is strictly positive for even P
- SL Lobatto and SL Newton-Cotes: strictly positive for odd P
- TL not robust for $P > 1$

Accuracy

- TL and SL Newton-Cotes converge $\left\| \widetilde{\psi} - \psi \right\|_{L^2}$ 2nd order for odd P, 3rd order for even P
- SL Lobatto and SL Gauss converge $\left\| \widetilde{\psi} - \psi \right\|_{L^2} \propto P + 1$

Outflow Robustness

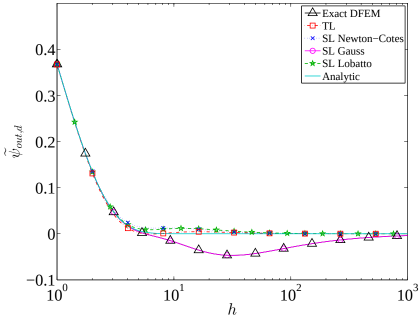

Figure: $P = 3$ Outflow as a function of h.

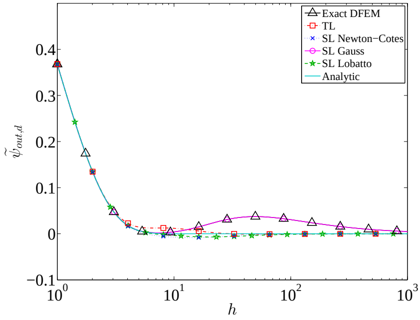

Figure: $P = 4$ Outflow as a function of h.

Order of Convergence

Convergence of $\left\|\widetilde{\psi} - \psi\right\|_{L^2}$ as a function of h

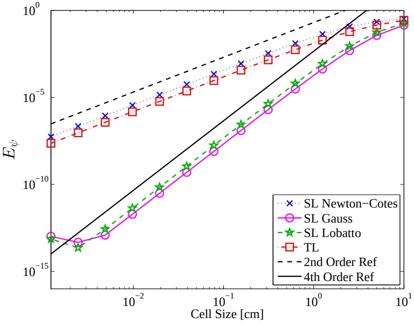

Figure: $P = 3$.

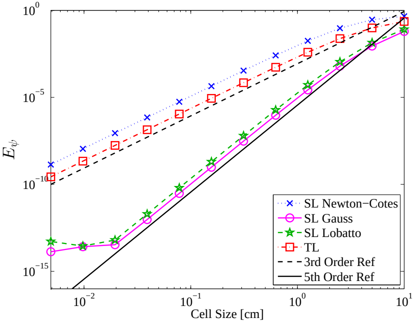

Figure: $P = 4$

New Results: Fixed Source Lumping (NS&E)

- Positivity of $\widetilde{\psi}(x)$ near inflow in source driven problem.
- Vacuum, no incident flux
- δ shaped source
- Exact integration of RHS source moments is the most robust

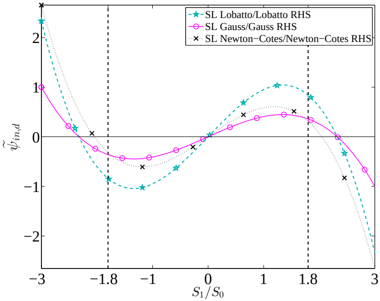

Figure: Numerical solution near cell inflow.

Motivation to Account for Cross Section Spatial Variation

- Many problems of interest to the NE community have within cell spatially varying cross section/opacity
  - Cross sections are functions of temperature, density, fuel burn-up, etc.
  - High fidelity simulations do not assume cell-wise constant values for these variables
- Neutronics examples: fuel depletion problems, coupled reactor physics...
- Radiative transfer: $\sigma = T^{-3}$

History

- Neutronics calculations almost exclusively approximate cross section as a cell-wise constant
  - Some work has focused on assuming cross section is a linear function within cells
  - Focus of this historical work has been on reproducing fine mesh results with coarser zoning
- Radiative transfer/radiative diffusion calculations (sometimes) account for within cell variation by using vertex based quadrature integration
  - Idea introduced by Adams and Nowak circa 1997
  - Used by some (ex. Ober and Shadid 2004)
  - Not by everyone

SL Schemes for Spatially Varying Cross Section Problems

- Trivial to extend quadrature integration to include spatial variation of cross section

$$\mathbf{R}_{\sigma,ij} = \begin{cases} \frac{\Delta x}{2}\sigma(s_i)w_i & i=j \\ 0 & \text{otherwise} \end{cases}$$

  where the DFEM equations that account for cross section spatial variation are:

$$\mu_d \mathbf{L}\vec{\psi}_d + \mathbf{R}_{\sigma_t}\vec{\psi}_d = \frac{1}{2}\mathbf{R}_{\sigma_s}\vec{\phi} + \vec{q}_d + \psi_{in}\vec{f}$$

- M&C 2013 showed that exact mass matrix integration not required for full order accuracy schemes
  - SL Lobatto does not exactly integrate **M** but has the same order of L^2 as SL Gauss

Test Problem

- Spatially varying cross section of the form:

$$\sigma_t(x) = c_1 e^{c_2 x}$$

- Incident flux, $\psi_{in,d}$ on the left, vacuum on the right, no sources.
- Analytic Solution

$$\psi(\mu_d, x) = \psi_{in,d} \exp\left[\frac{c_1}{\mu_d c_2}\left(1 - e^{c_2 x}\right)\right]$$

Additional Numerical Schemes

In addition to the self-lumping schemes, we will consider the following as well:

- **CXS DFEM**: Equally-spaced interpolation points, analytic integration approximate cross section by cell average value
- **EXS DFEM**: Equally-spaced interpolation points, (nearly) exact integration of cross section spatial dependence in the mass matrix

We will no longer consider the TL scheme.

New Result: Robustness Is Not Guaranteed

For an arbitrarily varying spatial cross section:

- Only linear SL Lobatto/SL Newton-Cotes yields strictly positive outflow:

$$\widetilde{\psi}_{out} = \frac{2\mu_d^2 \psi_{in,d}}{2\mu_d^2 + \Delta x^2 \Sigma_{t,1}\Sigma_{t,2} + \Delta x \mu_d \Sigma_{t,1} + \Delta x \mu_d \Sigma_{t,2}}$$

- Angular flux outflow for all schemes that explicitly account for cross-section spatial variation is a function of cell optical thickness **and** cross section spatial shape
- Dependence on anything other than optical thickness is non-physical!

Robustness-2

Outflow for exponential $\sigma_t(s)$, constant optical thickness of 20 MFP, $\mu_d = 1$, $x \in [0, 1\ cm]$.

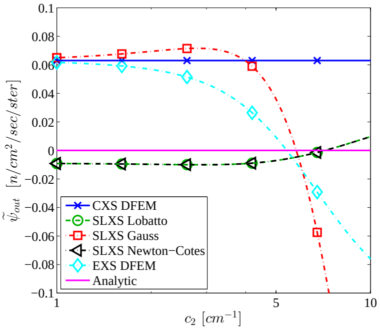

Figure: Quadratic Trial Space.

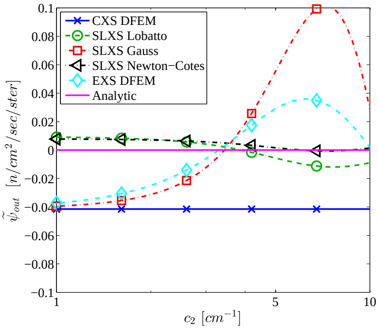

Figure: Cubic Trial Space.

Convergence Results

We examine the convergence of E_{ψ} and $E_{\psi_{out}}$ for a pure absorber with

$$\sigma_t(x) = 0.1 \ 10^{2x}$$

and $x \in [0, 1 \ cm]$. We define the error quantities as:

$$\begin{aligned} E_{\psi} &= \left\| \widetilde{\psi}_d(x) - \psi(x, \mu_d) \right\|_{L^2} \\ E_{\psi_{out}} &= \sqrt{\sum_{i=1}^{N_{cells}} \Delta x_i \left(\widetilde{\psi}_{out,i} - \psi(x_{i+1/2}) \right)^2} \end{aligned}$$

L^2 Convergence

New Result: SL Lobatto and SL Gauss are accurate methods for spatially varying cross section problems

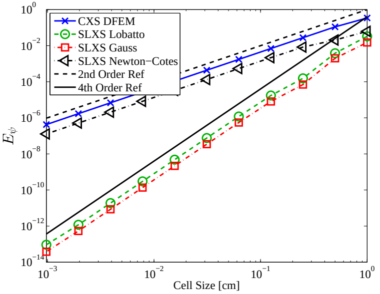

Figure: $P = 3$ convergence plot.

Summary of Convergence Orders

- SL Gauss: $\propto P + 1$
- SL Lobatto: $\propto P + 1$, less accurate than SL Gauss
- SL Newton-Cotes: 2 if odd P, 3 if even P
- CXS DFEM: 2 regardless of P

$E_{\psi_{out}}$ Convergence

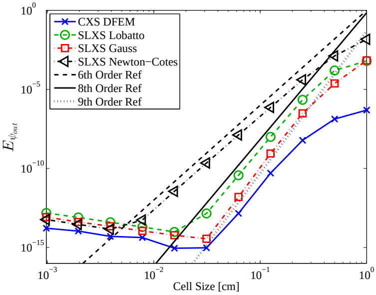

Figure: $P = 4$ convergence plot.

Summary of Convergence Orders

- SL Gauss: $2P + 1$
- SL Lobatto: $2P$
- SL Newton-Cotes: $P + 1$ for odd P, $P + 2$ for even P
- CXS DFEM: $2P + 1$

Interaction Rate

- Analytic interaction rate

$$IR(x) = \sigma_t(x)\psi(x,\mu_d)$$

- CXS DFEM approximation

$$\widetilde{IR}(x) = \hat{\sigma}_t\widetilde{\psi}(x)$$

- SL schemes: Only point-wise knowledge of $\sigma_t(x)$ in DFEM equations
  - Integrals: evaluate $\widetilde{IR}(x)$ with quadrature restricted to interpolation points
  - Plotting purposes:

$$\widetilde{IR}(x) = \sum_{j=1}^{P+1}\sigma_{t,j}\psi_j B_j(s)$$

L^2 error of $\widetilde{IR}(x)$

New Result: SL Lobatto and SL Gauss Accurately Approximate $\widetilde{IR}(x)$

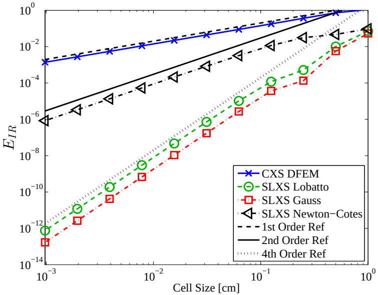

Figure: Cubic DFEM

Summary of Convergence Orders

- SL Gauss: $P+1$
- SL Lobatto: $P+1$
- SL Newton-Cotes: 2 for odd P, 3 for even P
- CXS DFEM: 1, regardless of trial space degree

E_{IR_A} Convergence

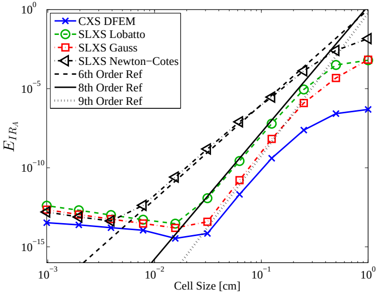

Figure: Quartic DFEM

Summary of Convergence Orders

- SL Gauss: $2P + 1$
- SL Lobatto: $2P$
- SL Newton-Cotes: $P + 1$ for odd P, $P + 2$ for even P
- CXS DFEM: $2P + 1$, regardless of trial space degree

CXS DFEM Accuracy Calculating IR_A

- How can CXS DFEM converge E_{IR_A} so accurately?
- Local Conservation

$$\text{Particles In} - \text{Particles Out} = \text{Total Interactions}$$

- Particles In: Outflow from Previous Cell
- Particles Out: Outflow from Current Cell
- CXS DFEM converges angular flux outflow $\propto 2P + 1$
- $\therefore$ CXS DFEM accurately calculates

$$\text{Total Interactions} = \Delta x \left(\widetilde{IR}_A \right)$$

CXS DFEM Interaction Rate Profile

New to Dissertation

Observation and explanation of blading phenomena

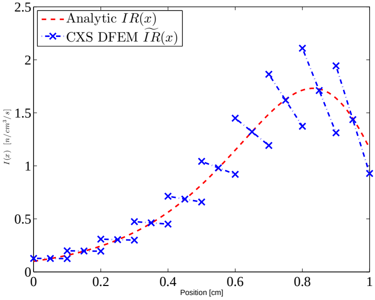

Figure: $\widetilde{IR}(x)$ profile.

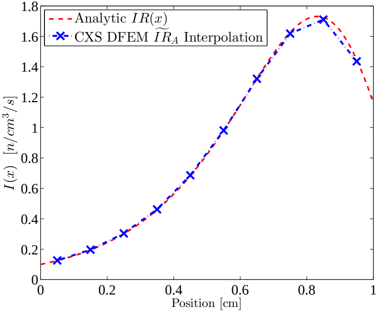

Figure: Interpolated $\widetilde{IR}_A$ profile.

Something Wrong with DFEM?

No. Consider the analytic solution to a problem that has the cell-wise average cross section.

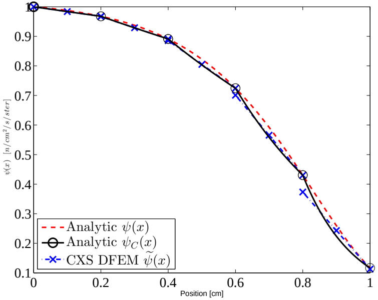

Figure: Angular Flux.

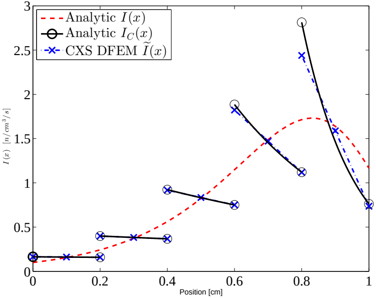

Figure: Interaction Rate.

Linear SL Lobatto Solution

New to Dissertation

New: Self-lumping schemes do not exhibit blading

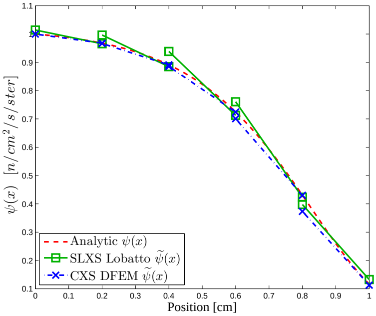

Figure: Angular Flux.

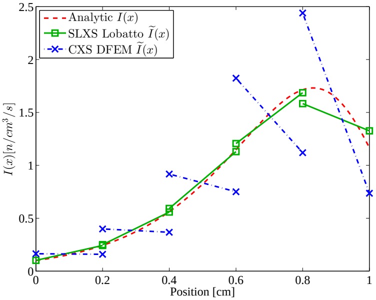

Figure: Interaction Rate.

Grey, Spatially Analytic Radiative Transfer

$$\frac{1}{c\Delta t}\left(I^{n+1} - I^{n}\right) + \mu\frac{\partial}{\partial x}I + \sigma_t^{n+1}I^{n+1} = \frac{\sigma_s^{n+1}}{4\pi}\phi^{n+1} + \sigma_a B(T^{n+1})$$

$$\frac{C_v}{\Delta t}\left(T^{n+1} - T^{n}\right) = \sigma_a^{n+1}\left(\phi^{n+1} - 4\pi B(T^{n+1})\right)$$

Linearizing the Plank function about an arbitrary temperature, T^*:

$$\frac{1}{c\Delta t}\left(I^{n+1} - I^{n}\right) + \mu\frac{\partial}{\partial x}I^{n+1} + \sigma_t^{n+1}I^{n+1} = \frac{\sigma_s^{n+1}}{4\pi}\phi^{n+1} + \sigma_a^{n+1}\left[B(T^*) + \left.\frac{\partial B}{\partial T}\right|_{T=T^*}(T^{n+1} - T^*)\right] \quad (1)$$

$$\frac{C_v^{n+1}}{\Delta t}\left(T^{n+1} - T^{n}\right) = \sigma_a^{n+1}\phi^{n+1} - 4\pi\sigma_a^{n+1}\left[B(T^*) + \left.\frac{\partial B}{\partial T}\right|_{T=T^*}(T^{n+1} - T^*)\right] \quad (2)$$

Spatially Discretized Radiative Transfer

Drop $^{n+1}$ and discretize Eq. (1) and Eq. (2) with P degree DFEM.

$$\frac{1}{c\Delta t}\mathbf{M}\left(\vec{I}-\vec{I}^n\right)+\mu\mathbf{L}\vec{I}+\mathbf{R}_{\sigma_t}\vec{I}= \frac{1}{4\pi}\mathbf{R}_{\sigma_s}\vec{\phi}+\mathbf{R}_{\sigma_a}\left[\vec{B^*}+\mathbf{D}(\vec{T}-\vec{T^*})\right]+\vec{f}I_{in} \quad (3)$$

$$\frac{1}{\Delta t}\mathbf{R}_{C_v}\left(\vec{T}-\vec{T}^n\right)=\mathbf{R}_{\sigma_a}\left\{\vec{\phi}-4\pi\left[\vec{B^*}+\mathbf{D}(\vec{T}-\vec{T^*})\right]\right\} \quad (4)$$

Define $(P+1)\times(P+1)$ diagonal matrix $\mathbf{D}$ and $(P+1)\times 1$ vector $\vec{B^*}$:

$$\mathbf{D}_{ii} = \left.\frac{\partial B}{\partial T}\right|_{T=T_i^*}$$

$$\vec{B^*}_i = B(T_i^*)$$

Solving for $\vec{T}$

Solve Eq. (4) for $\vec{T}$, use in Eq. (3) to eliminate T^{n+1} dependence.

$$\left[\mathbf{I} + 4\pi\Delta t \mathbf{R}_{C_v}^{-1}\mathbf{R}_{\sigma_a}\mathbf{D}\right]\vec{T} = \vec{T^n} + \Delta t \mathbf{R}_{C_v}^{-1}\mathbf{R}_{\sigma_a}\vec{\phi} \\ - 4\pi\Delta t \mathbf{R}_{C_v}^{-1}\mathbf{R}_{\sigma_a}\left[\vec{B^*} - \mathbf{D}\vec{T^*}\right]$$

Adding "zero" to both sides

$$= +\mathbf{I}\left[\vec{T^*} - \vec{T^*}\right]$$

Get a Newton update for $T^{(\vec{n+1})}$

$$\vec{T} = \vec{T^*} + \left[\mathbf{I} + 4\pi\Delta t \mathbf{R}_{C_v}^{-1}\mathbf{R}_{\sigma_a}\mathbf{D}\right]^{-1}\left[\left(\vec{T^n} - \vec{T^*}\right)\right] + \\ \left[\mathbf{I} + 4\pi\Delta t \mathbf{R}_{C_v}^{-1}\mathbf{R}_{\sigma_a}\mathbf{D}\right]^{-1}\Delta t \mathbf{R}_{C_v}^{-1}\mathbf{R}_{\sigma_a}\left[\vec{\phi} - 4\pi\vec{B^*}\right] \quad (5)$$

Forming the Radiation Equation

1. Eq. (5) is inserted into the radiation equation, Eq. (3)
2. The only unknown in this new equation is $\vec{I}^{n+1}$
   - Opacities are evaluated at $\vec{T}^*$
3. Eq. (5) becomes a Newton iteration for $\vec{T}^*$
4. Cannot isolate $\vec{T}^{n+1}$ if $\frac{\partial \sigma}{\partial T}$ terms accounted for
5. No observed stability/convergence issues with updating σ in a fixed-point style
6. New radiation equation (next slide) can be written in pseudo-fission format
   - DFEM unknowns de-couple with SL schemes (diagonal $\mathbf{R}$)

Pseudo-Fission Form of Radiation Equation

$$\mu \mathbf{L}\vec{I} + \mathbf{R}_{\sigma_\tau}\vec{I} = \frac{1}{4\pi}\mathbf{R}_{\sigma_s}\vec{\phi} + \frac{1}{4\pi}\bar{\bar{\nu}}\mathbf{R}_{\sigma_a}\vec{\phi} + \bar{\xi} + \vec{f}I_{in} \tag{6}$$

Where we have made the following definitions:

$$\begin{aligned}
\mathbf{R}_{\sigma_\tau} &= \frac{1}{c\Delta t}\mathbf{M} + \mathbf{R}_{\sigma_t} \\
\bar{\bar{\nu}} &= 4\pi\mathbf{R}_{\sigma_a}\mathbf{D}\left[\mathbf{I} + 4\pi\Delta t\mathbf{R}_{C_v}^{-1}\mathbf{R}_{\sigma_a}\mathbf{D}\right]^{-1}\Delta t\mathbf{R}_{C_v}^{-1} \\
\bar{\xi} &= \mathbf{R}_{\sigma_a}\vec{B}^* + \mathbf{R}_{\sigma_a}\mathbf{D}\left[\mathbf{I} + 4\pi\Delta t\mathbf{R}_{C_v}^{-1}\mathbf{R}_{\sigma_a}\mathbf{D}\right]^{-1}\left[\vec{T}^n - \vec{T}^*\right] \\
\ldots & -4\pi\mathbf{R}_{\sigma_a}\mathbf{D}\left[\mathbf{I} + 4\pi\Delta t\mathbf{R}_{C_v}^{-1}\mathbf{R}_{\sigma_a}\mathbf{D}\right]^{-1}\Delta t\mathbf{R}_{C_v}^{-1}\mathbf{R}_{\sigma_a}\vec{B}^*
\end{aligned}$$

DOE CSGF

SL Lobatto Radiative Transfer Solution

New to Dissertation

Observation of radiative transfer temperature blading, explanation of why, and a viable solution to the problem

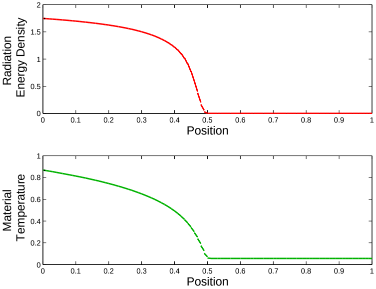

Figure: Linear SL Lobatto solution to the Marshak wave problem.

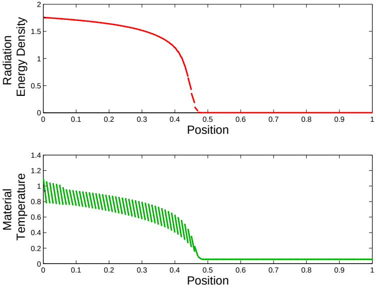

Figure: Linear, traditional lumping, constant cross section solution to the Marshak wave problem.

Third Known Use of MIP DSA!

Neutronics Spectral Radius Test:

- Slab, 80 [cm] thick
- $\sigma_t = 10$ [cm^{-1}]
- $c = 0.9999$
- S_{16} quadrature
- Random initial solution

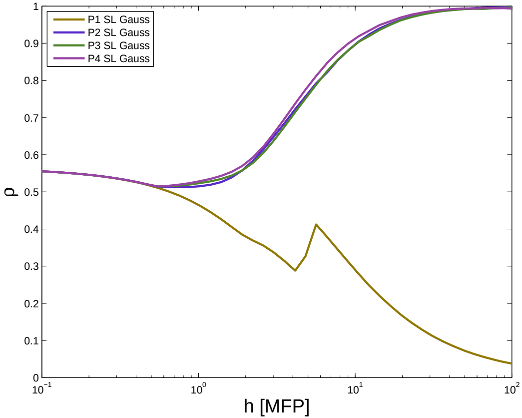

Figure: Numerical SPR for P degree SL Gauss transport with $P = 1$ SL Gauss MIP DSA

Krylov with Low Order MIP

- 80 [cm] slab
- $\sigma_t = 10$ [cm^{-1}]
- $c = 0.9999$
- S_{16} quadrature
- Uniform, isotropic source, vacuum BC

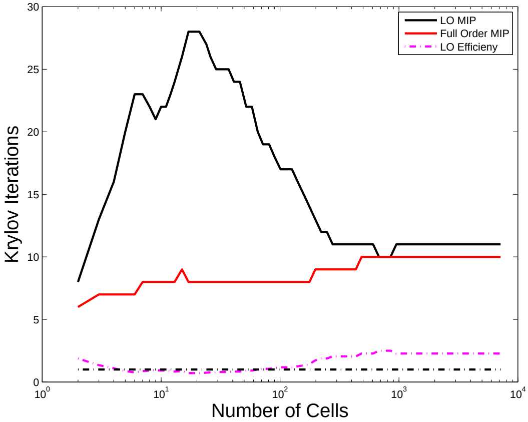

Figure: $P = 4$ SL Gauss transport

Work to Be Completed

Slab, Multi-frequency S_N Radiative Transfer Code

- C++
- Arbitrary trial space degree
- Lobatto, Gauss, and equally-spaced interpolation points
- Arbitrary SDIRK time integration
- Fixed-point and Krylov for solving within group scattering
- Fixed-point and Krylov for absorption/re-emission iteration
- MIP DSA/LMFGA operators
- Use PETSc / Trillinos for GMRES and inverting diffusion operators

Complete non-negative, unstructured mesh bilinear DFEM implementation in PDT (98% done)

Questions?